WARSAW UNIVERSITY OF TECHNOLOGY Index 351733
FACULTY OF CIVIL ENGINEERING
COMMITTEE FOR CIVIL AND WATER ENGINEERING
POLISH ACADEMY OF SCIENCES ISSN 1230-2945

DOI: 10.24425/ace.2022.141909

ARCHIVES OF CIVIL ENGINEERING

Vol. LXVIII ISSUE 3 2022

pp. 661 –677

Research paper

Centrifuge model test of parallel shield underneath high-speed railway tunnel

Ruizhen Fei[1], Limin Peng[2], Chunlei Zhang[3], Jiqing Zhang[4], Peng Zhang[5]

Abstract: In order to study the ground disturbance and the influence relationship between the two tunnels during the construction of the new shield tunnel undercrossing the existing high-speed railway tunnel, the centrifuge test was used to simulate the construction of the parallel shield tunnel undercrossing the high-speed railway tunnel, and the variation law of the internal force, segment deformation and surface settlement of the existing high-speed railway tunnel undercrossing the shield was studied. It is found that the adverse effects caused by the later tunnel are less than those caused by the first tunnel excavation. For the existing tunnels without settlement joints, the longitudinal settlement of the inverted arch and the vault is U-shaped and anti-U-shaped respectively. The settlement value of the ground surface and the existing tunnel is increased by more than 100%. When the shield passes through the high-speed railway tunnel, the transverse bending strain is larger than the longitudinal, and special attention should be paid at the corner.

Keywords: twin-tunnel excavation, settlement joint, centrifuge test, tunnel lining

[1]PhD., Eng., Central South University, School of Civil Engineering, Changsha, 410075, China; China Railway Design Corporation, Tianjin, 300142, China, e-mail: fruizhen@163.com, ORCID: 0000-0002-9142-4890
[2]Prof., PhD., Central South University, School of Civil Engineering, Changsha, 410075, China, e-mail: lmpeng@mail.csu.edu.cn, ORCID: 0000-0002-0402-2368
[3]MSc., Eng., China Railway Design Corporation, Tianjin, 300142, China, e-mail: zhangchunlei@crdc.com, ORCID: 0000-0002-0630-1467
[4]MSc., Eng., China Railway Design Corporation, Tianjin, 300142, China, e-mail: zhangjiqing@crdc.com, ORCID: 0000-0002-0864-9934
[5]MSc., Eng., China Railway Design Corporation, Tianjin, 300142, China, e-mail: zhangpeng04@crdc.com, ORCID: 0000-0001-6185-2379

1. Introduction

With the rise of urban subway construction and the shortage of underground space resources, the construction of urban subway tunnels will inevitably cross the existing tunnels. Tunnel excavation disturbs the surrounding rock and transmits it to the existing tunnel to cause tunnel deformation and cracking, thereby affecting the normal use and structural safety of the existing tunnel. Therefore, studying the interaction mechanism of tunnel-surrounding rock-tunnel and evaluating the influence of new tunnel construction on existing tunnel is an important foundation to ensure the safety of existing tunnel and new tunnel construction.

Some reasearch carried out the model test above the tunnel under the condition of 1 g, the results show that the new tunnel excavation is the stress redistribution of the existing tunnel lining, and then the existing tunnel lining has undergone significant deformation [1]. Although there are many achievements in the model test of shield excavation under the condition of 1 g, the stress level of 1 g test is small, so it cannot reproduce the characteristics of the prototype. The only way to solve this problem is to improve the self-weight of the model and make it equivalent to the prototype. Centrifugal model test can achieve this equivalence , which has become an important way to solve the boundary value problem of complex geotechnical engineering [2].

For tunnel vertical crossing carried out geotechnical centrifugal model tests [3–5]. In particular, model tests using centrifuges, studied the response of the existing tunnel to the new tunnel under different column depths under the condition of sand acceleration of 60 g [2]. They found that the maximum settlement of an existing funnel was 50 percent greater at a column aspect ratio of 0.5 than at a column aspect ratio of 2.0. The existing tunnel extends horizontally with a P/D of 0.5 and vertically with a PID of 2.0. Numerical back analysis shows that when P/D is 0.5, the stress reduction in horizontal direction of the existing tunnel is greater than that in vertical direction. Therefore, centrifuge testing can provide high-quality and reliable data for the calibration of numerical models, which can be used for numerical studies. Ng, et al. [2, 3] and Bonyarak and Ng [6] conducted a systematic study on the interaction between vertical tunnels. They conducted a series of centrifugal tests to determine the effects of volume loss, weight loss, pillar depth, tunnel shield, cover depth (distance from tunnel crown to ground) and construction sequence on tunnel-tunnel interaction.

Numerical analysis has been used to study double tunnel interactions. Addenbrooke and Potts 2001 [7] carried out finite element analysis of parallel tunnels side by side or back to back in London Clay. Parallel tunnels are simulated under plane strain conditions. For the side-by-side geometry, the diameter of the first tunnel is lengthened horizontally and shortened vertically through the second tunnel. When the pillar width is greater than 7 diameter, the influence of the second tunnel on the first tunnel decreases. In the bearing geometry, the deformation of the lining of the existing tunnel is more serious if the secondary excavation occurs under the existing tunnel. When the pillar depth is greater than 3 diameters, this interaction is negligible. The results show that when a new tunnel passes through an existing tunnel within 3 diameters, the interaction between tunnels should be

fully considered. On the basis of the settlement of ground and foundation, the influence of shield tunnel construction is evaluated. Combined with field monitoring data, the polynomial formula for predicting the depth and shape of asymmetric settlement trough in double-track tunnel is determined [8]. Shield tunneling in urban areas is easy to cause surface subsidence. Combined with engineering examples, the key construction technology, construction control parameters and matters needing attention in the construction period of shield machine are analyzed [9]. Zhang and Huang [10] studied the soil disturbance and the deformation of existing parallel double-circular tunnels caused by up-crossing and down-crossing circular tunnels through three-dimensional finite element numerical simulation. The deformation of existing tunnels is mainly caused by undercrossing tunnels. In all these studies, the existing tunnel and the new tunnel share similar geometric shapes (i.e., circular and ordinary sizes). However, encountering horseshoe tunnels is not uncommon.

In fact, the stress redistribution and deformation of horseshoe tunnel may be more severe than circular tunnel [11]. Some scholars carried out field research to investigate the excavation effect of bias double-arch tunnel. Their effects on the excavation of unsymmetrically loaded multi-arch tunnels are inconsistent, possibly due to the lack of complete and reliable data [12, 13].

In recent years, the longitudinal and circumferential joints of tunnels have attracted much attention [14–16]. However, there is little research on settlement joints (i.e. a completely disconnected gap filled with flexible adhesive materials), even if such joints can significantly reduce the longitudinal bending stiffness of tunnels. The interaction between circular and non-circular jointed tunnels has been widely reported in the literature, and the influence of joints on the interaction is not clear.

In this paper, through the three-dimensional centrifuge model test, the influence of the construction of the new parallel shield tunnel on the existing horseshoe tunnel is studied. The tunnel response caused by each new tunnel is emphatically studied, and the influence of the settlement joint of the existing tunnel is investigated. In order to provide reference for future cross tunnel design and construction.

2. Three-dimensional centrifuge test

The centrifuge model test was completed on the centrifuge of Hong Kong University of Science and Technology, Fig. 1 is the photo of the geotechnical centrifuge. The capacity is 400 g-t, the rotation radius is 4.2 m, the maximum acceleration is 150 g, and the three-dimensional model box size is 1.25 m (length) $\times$ 0.93 m (width) $\times$ 0.85 m (height).

2.1. Experiment conditions

The new tunnel and the existing tunnel are simulated by aluminum pipeline, and the soil is selected with Toyoura sand [17] with small particle size (average particle size is 0.17 mm) [18] to reduce the influence of particle size on tunnel-soil structure interaction. The experiment consists of two groups. In Test 1, considering the overall lining structure

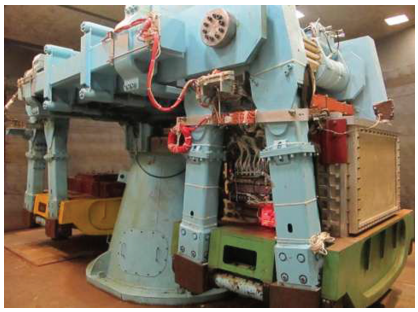

Fig. 1. Photo of geotechnical centrifuge

of Liuyanghe tunnel, the influence of double-line shield construction on the built tunnel was studied under dry sand conditions. Test 2 completely cuts the existing tunnel along the middle line and ensures that there is no connection between the two tunnels to simulate the structure of the settlement joint in the actual project. Other parameters are the same as those in Test 1. The influence of the newly excavated tunnel on the built tunnel under the condition of the settlement joint is studied.

As mentioned above, the test methods and configuration modes of Test 1 and Test 2 are the same, and the only difference is that Test 2 sets a sink joint. In order to facilitate the description, the description of the test design is mainly Test 1.

2.2. Test parameters

The gravity acceleration of this centrifuge test is 60 times under normal gravity field, so the model size is 1/60. The total size of the test model is 1.25 m (length)×0.93 m (width)× 0.85 m (height). Fig. 2 shows the schematic diagram of the model section, in which the

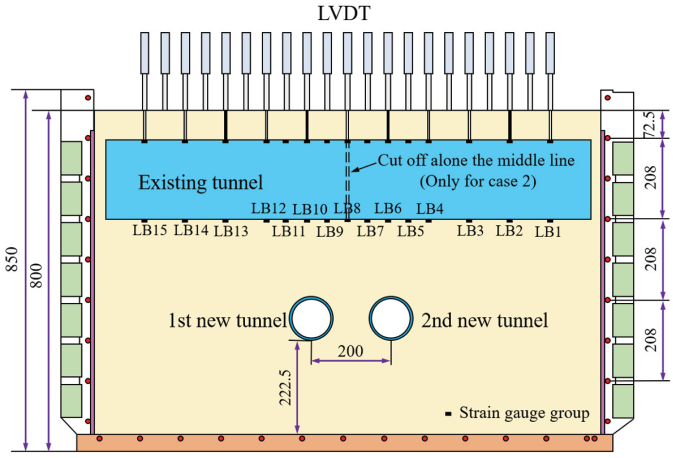

Fig. 2. Schematic diagram of centrifuge test model

layout positions of LVDT used to measure surface settlement and tunnel settlement are shown respectively. At the same time, a total of 15 sets of semiconductor strain gauges are arranged along the longitudinal direction of the tunnel to measure the longitudinal bending moment of the tunnel. The depth of Toyoura sandy soil layer is 800 mm, corresponding to the soil layer thickness of 48 m. The buried depths of the built tunnel and the newly excavated tunnel are 72.5 mm and 477.5 mm, respectively, corresponding to 4.35 m and 28.65 m in the field. The section heights of the existing tunnel and the newly excavated tunnel are 184.6 mm and 100 mm, respectively, corresponding to 11.1 m and 6 m on site.

2.3. Model materials and simulation system of formation loss

(1) Soil material

Toyoura sand was used as the test soil. The specific gravity of the sand is 2.65, the average particle diameter D_{50} is 0.17 mm, the maximum void ratio emax is 0.977, the minimum void ratio emin is 0.597, and the critical state friction angle $\varphi'_{cv} = 31°$ [19]. Quartz is the main mineral of Toyoura sand, which is crushed under high pressure (higher than 4000 kPa). Therefore, it is not necessary to consider the change of sand properties caused by crushed sand particles. The relative density of Toyoura sand measured in the two tests was 62%.

(2) Tunnel segments

The tunnel segments in the test are simulated by aluminum alloy tubes with a Young's modulus of 70 GPa. The size of the model tunnel is determined according to the similarity ratio (EI) of bending stiffness. The prototype of the tunnel is Liuyang River reinforced concrete tunnel of Wuhan-Guangzhou high-speed railway.

(3) Simulation system of formation loss

In this test, the drainage method was used to simulate the stratum loss caused by tunnel construction. Fig. 3 shows the section of the newly excavated tunnel. As shown in the figure,

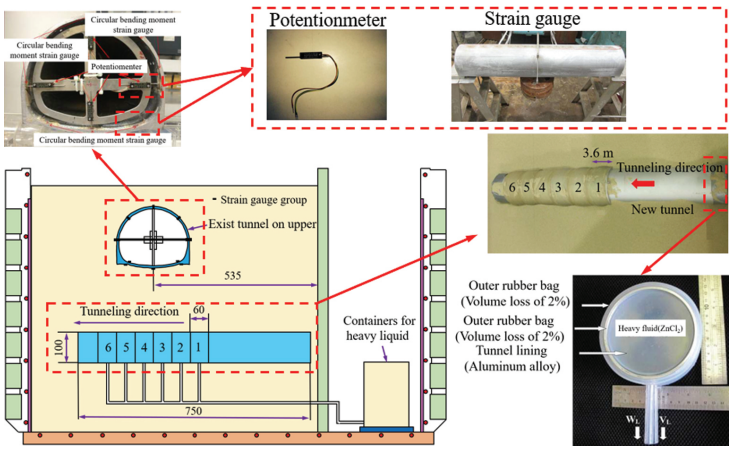

Fig. 3. Simulation system test diagram of formation loss

there is a rubber bag inside and outside the tunnel lining. During the test, the rubber bag will be filled with zinc chloride solution. The solution is approximately incompressible, and the density is close to that of sand in the test. In centrifuge test, the simulation of tunnel excavation is realized by releasing zinc chloride solution in one rubber bag inside and outside the tunnel lining. By releasing the solution outside the tunnel lining, the ground loss caused by tunnel excavation can be simulated (2%). The self-weight loss in tunnel can be simulated by releasing the solution in tunnel lining. A set of strain gauges are arranged every 45° along the transverse direction of the tunnel to measure the circumferential bending moment of the tunnel lining. In addition, four potentiometers are arranged to measure the vertical and horizontal inner diameter changes of the built tunnel.

2.4. Preparation of model box

Sand rain method was used to spread sand in the test, so that the sand was evenly distributed in the model box. Before the test, the height of sand, the height of existing tunnel and new tunnel and the relative density of sand were calibrated. The target relative density of Toyoura sand was 60% and the corresponding dry density was 1516 kg/m^3. At the same time, the new tunnel and the existing tunnel are temporarily fixed at the target height.

When sand is spread to 222.5 mm from the bottom of the model box, the new tunnel is arranged in parallel with the sand plane according to the designed spacing, as shown in Fig. 4. After the placement of the model, the sand was continued to the height of the new tunnel, and then the temporary fixation of the existing tunnel was lifted. For Test 2, the existing tunnel was completely cut off at the middle line, and the two tunnels were connected by four thin aluminum plates as temporary connections before the test to be conveniently put into the model box. As shown in Fig. 5, Fig. 5a shows the overall picture of the cut existing tunnel, and Fig. 5b shows the connection details between the two sections of the cut existing tunnel. After putting the existing tunnel into the model box and fixing

Fig. 4. The sand layer reaches the center line of the tunnel to be excavated

its position, the screws of all the fixed thin aluminum plates were loosened to remove the connection between the two tunnels. Then, continue to spread sand until the sand layer height reaches 800 mm. The resulting model box is shown in Fig. 6.

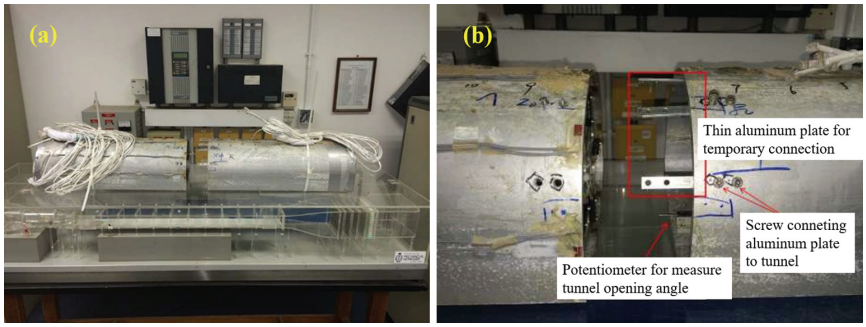

Fig. 5. Settlement joints of existing tunnels: (a) Global view of exisiting tunnel lining; (b) local view of exisiting tunnel lining

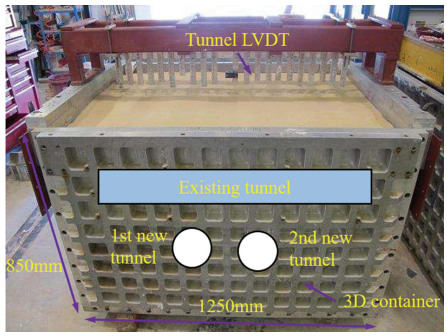

Fig. 6. Schematic diagram of centrifuge model test box on site

2.5. Test process

The test is divided into five stages: the centrifuge acceleration rises to 60 g, after the measurement data reading is stable, the air valve is opened, and the liquid in the water belt is gradually released to simulate the tunneling process of the tunnel. After the zinc chloride solution in each water-saving bag is released, wait for 2 minutes and release the next section. Fig. 7 shows the overlooking view of the centrifuge test model. The excavation process of the newly excavated tunnel is simulated by the method of discharging heavy liquid. The excavation sequence is 1L→2L→3L→4L→5L→6L→1R→2R→3R→4R→5R→6R, where 3L, 4L, 3L and 4L are directly below the constructed tunnel. In the test, the excavation length of each section is 60 mm, and the corresponding site is 3.6 m. The lower side of the model box is a reserved square slot for placing the control valves and heavy liquid storage tanks necessary to simulate tunnel excavation.

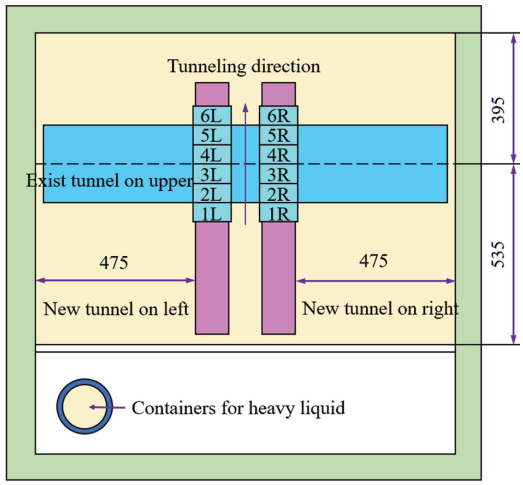

Fig. 7. Simulation system diagram of formation loss

3. Model test results

3.1. Surface subsidence caused by double tunnel excavation (Test 1)

Figure 8 is the surface settlement curve after the completion of the left and right tunnel construction. In order to facilitate the analysis, X/Z is used for standardization (z = 520 mm). It can be seen from Fig. 8 that the maximum surface settlement caused by the excavation of the left tunnel is 10.3 mm. After the double tunnel excavation is completed, the final maximum surface settlement is 16.5 mm.

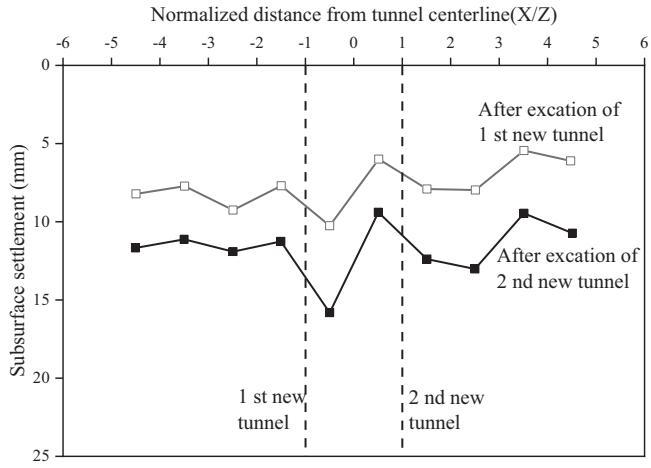

Fig. 8. Surface subsidence caused by double tunnel excavation

3.2. Settlement of Existing Tunnels Caused by Double Tunnel Excavation (Test 1)

Figure 9 is the settlement curve of existing tunnel caused by double tunnel excavation. Fig. 9 shows that the maximum existing tunnel settlement caused by the left tunnel excavation is 8.7 mm. After the double tunnel excavation is completed, the final maximum settlement of the existing tunnel is 13.5 mm.

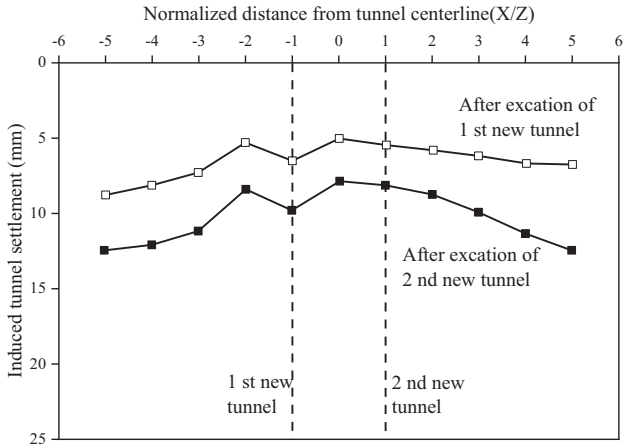

Fig. 9. Settlement of Existing Tunnel Caused by Double Tunnel Excavation

3.3. Longitudinal bending strain of existing tunnels induced by double tunnel excavation (Test 1)

Figure 10 shows the bending strain of the existing tunnel arch bottom caused by double shield excavation. It can be seen from the diagram that the calculated value and the measured value are slightly different, which may be due to the assumption that the existing tunnel is calculated according to the theory of the beam, resulting in inaccurate. However, the calculated values of longitudinal bending strain are in good agreement with the measured values, and the maximum values are basically the same.

As shown in Fig. 10, the bending positive strain occurs on both sides of the middle line of the existing tunnel, and the bending negative strain occurs on both ends of the existing tunnel. The change is basically consistent with the settlement curve of the arch bottom. After the left and right line shield excavation is completed, the total bending strain in the middle of the existing tunnel is $37.6\mu\varepsilon$, and the negative strains at both ends are $-9\mu\varepsilon$ and $-5\mu\varepsilon$, respectively. Considering that in ACI2001, the ultimate tensile strain (cracking) of unreinforced concrete is $150\mu\varepsilon$. In this test, the measured tensile strain is less than $150\mu\varepsilon$, because the size and thickness of the existing tunnel is very large, resulting in a more general tunnel (the left and right lines in this test) stiffness is much larger.

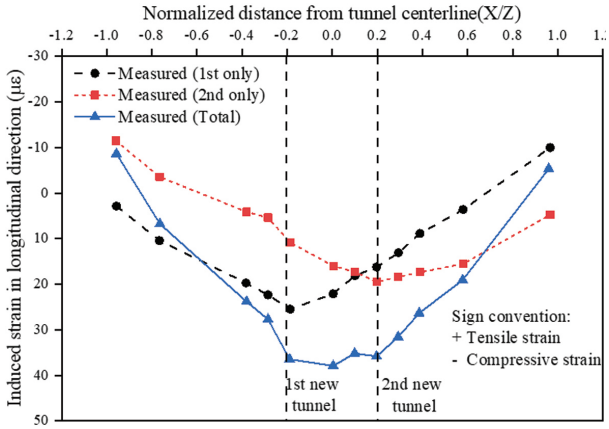

Fig. 10. Influence of double tunnel construction on longitudinal bending moment of existing tunnel

The maximum bending strain caused by the excavation of the left line is $25.2\mu\varepsilon$, which appears on the axis of the left line and gradually changes to $-8\mu\varepsilon$. The maximum bending strain caused by right line excavation is 11% smaller than that caused by left line excavation. The arch bottom settlement and longitudinal bending strain results of the existing line caused by the above double-line excavation mean that the influence of the right line of subsequent excavation on the existing tunnel is smaller, which is basically 5–11% smaller. The reason for this phenomenon is that after the left-line shield excavation is completed, the soil stress near the existing tunnel is redistributed. The first excavated left line reduces the soil stiffness in a small range near the excavated tunnel, because the constraint pressure near the tunnel is reduced. However, the stiffness of the adjacent soil is improved due to the increase of the constraint pressure, such as the soil near the existing tunnel and the subsequent excavation of the right-line tunnel, so the influence of the right-line excavation on the existing tunnel is smaller. The analysis of stress redistribution is not carried out here and can be found in study reported by Chen 2016 [20].

3.4. Distribution of circumferential bending moment at the central line of existing tunnels induced by double tunnel excavation (Test 1)

Figure 11 is the circumferential bending moment distribution map of the existing tunnel center line caused by double tunnel excavation. As shown in Fig. 11, the maximum and minimum transverse bending moments of the existing tunnel center line caused by left tunnel excavation are 62.1 and –14.4 kNm/m, respectively (positive value represents the lateral tension of the lining, negative value represents the lateral compression of the lining). After the double tunnel excavation is completed, the maximum and minimum transverse bending moments at the center line of the existing tunnel are 106.3 and –43 kNm/m, respectively.

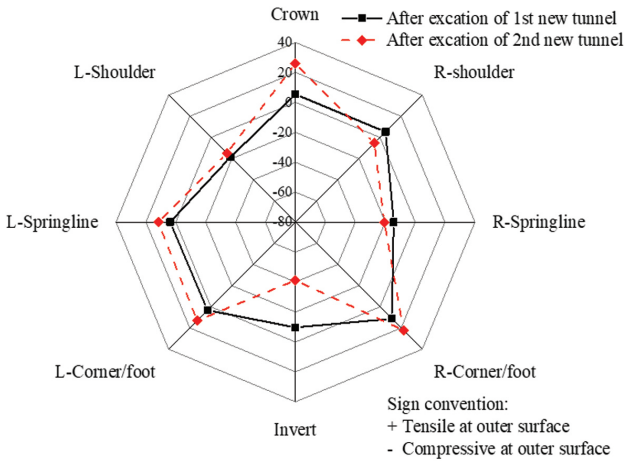

Fig. 11. Influence of Double Tunnel Construction on Lateral Moment of Existing Tunnel

3.5. Change of diameter at the center line of existing tunnel caused by double tunnel excavation (Test 1)

Figure 12 shows the change of the vertical and horizontal diameter at the center line of the existing tunnel caused by the excavation of the double tunnels, which are 3.7 mm and −4.8 mm (positive value represents elongation, and negative value represents shortening). After the double tunnel excavation is completed, the vertical and horizontal diameter changes at the center line of the existing tunnel are 8.1 mm and −8.5 mm, respectively.

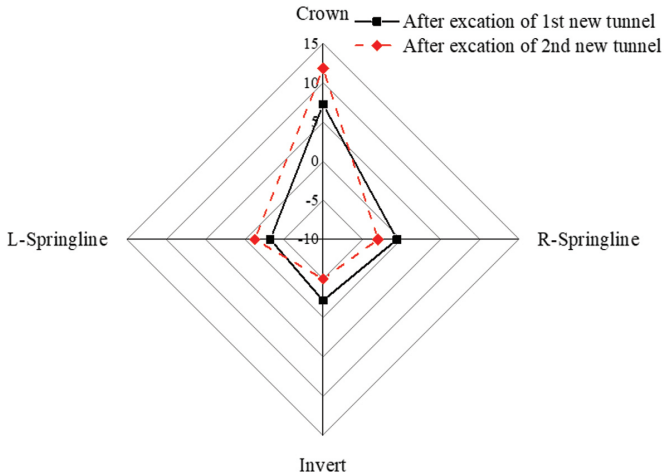

Fig. 12. Change of radius of existing tunnel center line caused by double tunnel construction

3.6. Effects of settlement joints on vault and ground settlement of existing tunnels (Tests 1 and 2)

Figure 13 compares the settlement of the surface and vault of the existing tunnel after the excavation of the double tunnels in Test 1 and Test 2. The surface settlement curve and vault settlement curve are both anti-U-shaped, which is because the coating layer of the existing tunnel is relatively thin, and the soil above the vault tends to have similar deformation with the vault. The maximum surface subsidence value is 12.4 mm, occurs at $X/Z = 0.9$, and gradually decreased to 9.8 mm, occurs at $X/Z = -0.1$. The surface settlement is larger than that of the vault, which means that the soil above the vault is compressed due to the excavation of the new left and right lines.

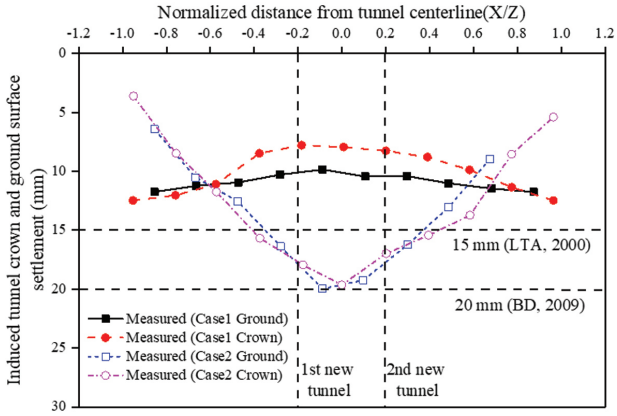

Fig. 13. Settlement of surface and vault of high-speed railway tunnel by double-line shield excavation

The surface subsidence in Test 2 showed a completely opposite trend to Test 1. The maximum and minimum values of ground settlement are 19.3 mm and 6 mm, respectively, and the positions are in the middle and both ends of the existing tunnel. The completely opposite ground settlement trend in Test 1 and Test 2 indicates that the shielding effect of the existing tunnel is eliminated by the settlement joint. The maximum vault settlement on the left side of the existing tunnel is 19.5 mm ($X/Z = -0.005$), 1.1 mm larger than that on the right side. This is consistent with the expectation. The previous study shows that the influence of the left line excavated first is greater than that of the right line excavated later. At the same time, the vault settlement value in Test 2 is 2.5 times of that in test 1.

3.7. Effect of settlement joints on longitudinal bending strain of tunnels (Tests 1 and 2)

Figure 14 shows the longitudinal bending strain of the existing tunnels in Test 1 and Test 2 after the excavation of the double tunnels. In Test 2, on the left side of the existing tunnel, the bending moment near the settlement joint should be zero. The maximum positive

bending moment strain occurs at the left axis, and the minimum negative bending moment occurs at $X/Z = -0.8$. The maximum bending positive strain is $4.6\mu\varepsilon$, and the negative strain is $-13.5\mu\varepsilon$. Similar distribution was also found on the right side of the existing tunnel, and the maximum bending positive and negative strains were $8\mu\varepsilon$ and $-15.4\mu\varepsilon$, respectively. However, in Test 1, most of the middle section of the existing tunnel is positive bending moment (from $X/Z = -0.8$ to 0.8), which should be attributed to its continuous bending stiffness. The maximum bending strain of $37.6\mu\varepsilon$ is 140% larger than that of test 2.

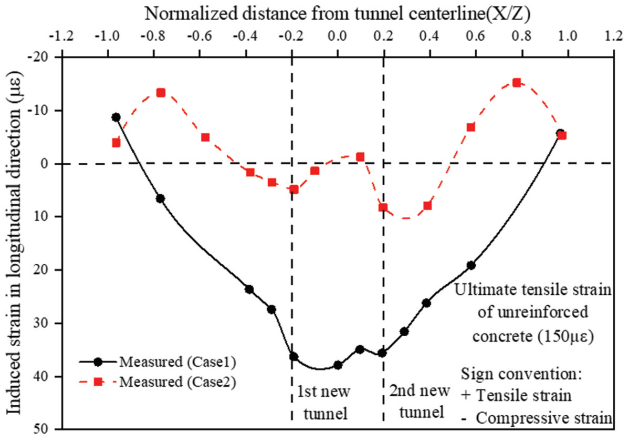

Fig. 14. Longitudinal bending strain of Test 1 and Test 2 high-speed railway tunnels after double-track shield excavation

Longitudinal shear stress can be calculated by bending moment. The maximum shear stress of test1 and test2 were 970 kPa and 260 kPa, respectively. Assuming that the allowable shear stress of concrete is 660 kPa (According to ACI2001 standard [21], the axial compressive strength of concrete, $f = 50$ MPa, reduction coefficient 0.55), the shear stress of concrete in Test 1 has exceeded the allowable value, and the existing tunnel may crack due to shear.

3.8. Effect of settlement joints on lateral response of tunnel (Test 1 and Test 2)

Figure 15 compares the radial displacements of existing tunnels in Test 1 and test 2. In Test 1, the existing tunnel diameter increases in the vertical direction and decreases in the horizontal direction. The radial measured values were 5 mm, 8.8 mm, –4 mm, –3.2 mm in vault, vault bottom, left side and right side respectively. In the second test, the existing tunnel also increases in the vertical direction and decreases in the horizontal direction. The radial measurement values in the vault, vault bottom, left and right sides are 5.2 mm, 8.4 mm, –5 mm, –4.1 mm, respectively, which are 104%, 95%, 125%, 125% of the first test.

Figure 16 shows the transverse bending strain of the existing tunnel after double tunnel excavation.

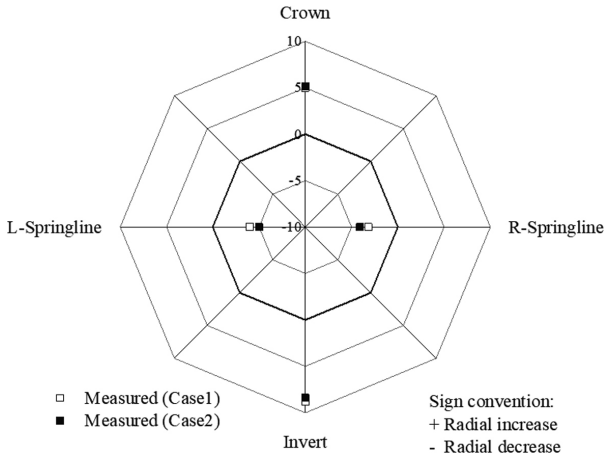

Fig. 15. Radial deformation of high-speed railway tunnel caused by double-track shield excavation

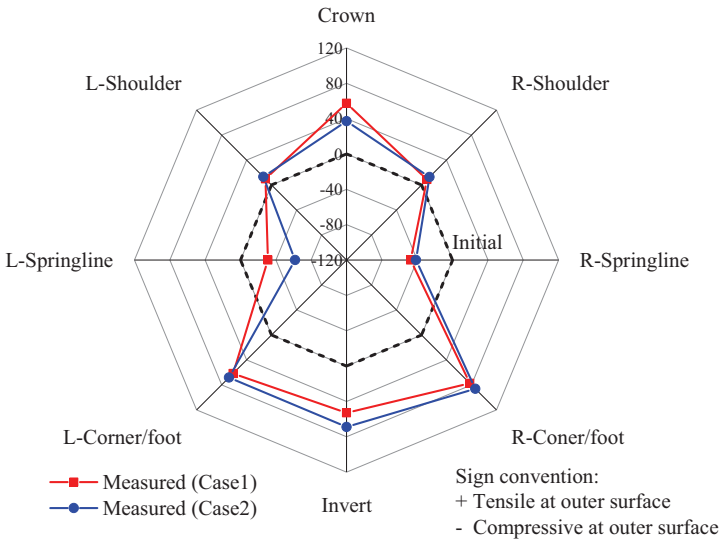

Fig. 16. Lateral bending strain of high-speed railway tunnel after double tunnel excavation

In the two tests, the bending strain measurement values of vault, arch bottom, shoulders and knees are positive, while the bending strain measurement values of the two arch positions are negative. This is consistent with the finding when the existing tunnel is vertically elongated and horizontally compressed. The maximum measured bending strain of Test 1 was 76.3$\mu\varepsilon$, and that of Test 2 was 85.6$\mu\varepsilon$, which was 12% larger. In both tests, the

maximum bending strain occurs at the lower right corner of the existing tunnel, meaning that this position may be the most dangerous position of the existing tunnel during double tunnel excavation.

4. Conclusions

Although the centrifugal test and numerical simulation are carried out according to the accurate size of the high-speed railway tunnel and the shield tunnel of Metro Line 3, the complex engineering geological and hydrogeological conditions in the field are not considered, so as to simplify the analysis and enable the testal analysis under dry sand conditions. This paper mainly studies the response of the excavation of the shield tunnel under the dry sand stratum to the existing tunnel. In practical engineering, the tunnel is usually below the groundwater level. During the shield construction, the seepage of the surrounding groundwater occurs, which affects the properties of the surrounding soil. Therefore, the following conclusions may not be suitable for direct application in engineering practice, mainly analyzing the data trend found in the test. Research conclusions also need to take seriously. From the results of centrifugal test, it is concluded that:

1. The arch bottom settlement and longitudinal bending strain of the high-speed railway tunnel caused by the subsequent right-line shield excavation are 5% and 11% smaller than those caused by the previous left-line shield excavation, respectively. Therefore, it is sufficient for the design to consider the most unfavorable influence of the previous shield excavation to the later shield excavation.
2. In the test without considering the settlement joints, the settlement curve of the arch bottom is U-shaped, but the settlement curve of the vault is anti-U-shaped. This is because the vertical deformation of the tunnel covers the settlement deformation of the arch bottom, which may be due to the larger size of the existing tunnel and the thinner cover thickness.
3. Consideration of settlement joints greatly reduces the shielding effect of high-speed railway tunnels. When considering the settlement joints, the vault and ground settlement of the existing tunnel increase by 100%, and the maximum longitudinal bending strain and shear stress decrease by 60%. This is because the settlement joint makes the bending stiffness of the existing tunnel greatly reduced.
4. The trend of transverse bending strain and deformation of high-speed railway tunnel considering the settlement joint is similar to that without considering the settlement joint, but the value is slightly larger.

Acknowledgements

This work was funded by the National Natural Science Foundation of China under Grant Nos. 51978669 and the China Railway Design Corporation Foundation under Grant Nos. 721239. The authors are grateful for the great support awarded.

References

[1] S.H. Kim, H.J. Burd, G.W.E. Milligan, "Model testing of closely spaced tunnels in clay", *Géotechnique*, 1998, vol. 48, no. 3, pp. 375–388, DOI: 10.1680/geot.1998.48.3.375.

[2] C.W.W. Ng, T. Boonyarak, D. Mašín, "Effects of Pillar depth and shielding on the interaction of crossing multitunnels", *Journal of Geotechnical and Geoenvironmental Engineering*, 2015, vol. 141, no. 6, DOI: 10.1061/(ASCE)GT.1943-5606.0001293.

[3] C.W.W. Ng, T. Boonyarak, D. Mašín, "Three-dimensional centrifuge and numerical modeling of the interaction between perpendicularly crossing tunnels", *Canadian Geotechnical Journal*, 2013, vol. 50, no. 9, pp. 935–946, DOI: 10.1139/cgj-2012-0445.

[4] C.W.W. Ng, R. Wang, T. Boonyarak, "A comparative study of the different responses of circular and horseshoe-shaped tunnels to an advancing tunnel underneath", *Géotechnique Letters*, 2016, vol. 6, no. 2, pp. 168–175, DOI: 10.1680/jgele.16.00001.

[5] C.Y. Gue, M.J. Wilcock, M.M. Alhaddad, et al., "Tunneling close beneath an existing tunnel in clay–perpendicular under crossing", *Géotechnique*, 2017, vol. 67, no. 9, pp. 795–807, DOI: 10.1680/jgeot.SiP17.P.117.

[6] T. Boonyarak, C.W.W. Ng, "Effects of construction sequence and cover depth on crossing-tunnel interaction", *Canadian Geotechnical Journal*, 2015, vol. 52, no. 7, pp. 851–867, DOI: 10.1139/cgj-2014-0235.

[7] T.I. Addenbrooke, D.M. Potts, "Twin tunnel interaction: surface and subsurface effects", *The International Journal of Geomechanics*, 2001, vol. 1, no. 2, pp. 249–271, DOI: 10.1061/(ASCE)1532-3641(2001)1:2(249).

[8] R. Kuszyk, A. Sieminska-Lewandowska, "Subsidence trough asymmetry calculations in twin tube TBM tunnelling", *Archives of Civil Engineering*, 2021, vol. 67, no. 2, pp. 675-689, DOI: 10.24425/ace.2021.137191.

[9] X.L. Ngueyen, L. Wu, K.T. Nguyen, et al., "Research on launching technology of shield tunnel in Ho Chi Minh Metro line 1", *Archives of Civil Engineering*, 2021, vol. 67, no. 1, pp. 387-401, DOI: 10.24425/ace.2021.136479.

[10] Z. Zhang, M. Huang, "Geotechnical influence on existing subway tunnels induced by multiline tunneling in Shanghai soft soil", *Computers and Geotechnics*, 2014, vol. 56, pp. 121–132, DOI: 10.1016/j.compgeo.2013.11.008.

[11] C. González-Nicieza, A.E. Álvarez-Vigil, A. Menéndez-Díaz, et al., "Influence of the depth and shape of a tunnel in the application of the convergence–confinement method", *Tunnelling and Underground Space Technology*, 2008, vol. 23, no. 1, pp. 25–37, DOI: 10.1016/j.tust.2006.12.001.

[12] L. Chen, "Effect of twin-tunnel excavation on existing horseshoe shaped tunnel", M.Philos. thesis, Hong Kong University of Science and Technology, 2016.

[13] X.G. Li, D.J. Yuan, "Response of a double-decked metro tunnel to shield driving of twin closely undercrossing tunnels", *Tunnelling and Underground Space Technology*, 2012, vol. 28, pp. 18–30, DOI: 10.1016/j.tust.2011.08.005.

[14] X. Huang, H. Huang, J. Zhang, "Flattening of jointed shield-driven tunnel induced by longitudinal differential settlements", *Tunnelling and Underground Space Technology*, 2012, vol. 31, pp. 20–32, DOI: 10.1016/j.tust.2012.04.002.

[15] F. Ye, C.F. Gou, H.D. Sun, et al., "Model test study on effective ratio of segment transverse bending rigidity of shield tunnel", *Tunnelling and Underground Space Technology*, 2014, vol. 41, pp. 193–205, DOI: 10.1016/j.tust.2013.12.011.

[16] J. Shi, C.W.W. Ng, Y. Chen, "Three-dimensional numerical parametric study of the influence of basement excavation on existing tunnel", *Computers and Geotechnics*, 2015, vol. 63, pp. 146–158, DOI: 10.1016/j.compgeo.2014.09.002.

[17] D.J. Goodings, D.R. Gillette, "Model size effects in centrifuge models of granular slope instability", *Geotechnical Testing Journal*, 1996, vol. 19, no. 3, pp. 277–285, DOI: 10.1520/GTJ10353J.

[18] S. Yamashita, M. Jamiolkowski, D.C.F. Lo Presti, "Stiffness nonlinearity of three sands", *Journal of Geotechnical and Geoenvironmental Engineering*, 2000, vol. 126, no. 10, pp. 929–938, DOI: 10.1061/(ASCE)1090-0241(2000)126:10(929).

[19] K. Ishihara, "Liquefaction and flow failure during earthquakes", *Géotechnique*, 1993, vol. 43, no. 3, pp. 351-415, DOI: 10.1680/geot.1993.43.3.351.

[20] R. Chen, X. Lin, X. Kang, et al., "Deformation and stress characteristics of existing twin tunnels induced by close-distance EPBS under-crossing", *Tunnelling and Underground Space Technology*, 2018, vol. 82, no. 12, pp. 468–481, DOI: 10.1016/j.tust.2018.08.059.

[21] ACI Committee, *ACI 318M-11 Building code requirements for structural concrete and commentary*. Farmington Hills, MI: ACI, 2001.

Received: 10.05.2022, Revised: 08.06.2022